[Frontiers in Bioscience 4904-4911, May 1, 2008]

Test systems for measuring ocular parameters and visual function in mice

Frank Schaeffel

Section of Neurobiology of the Eye, University Eye Hospital, Calwerstrasse 7/1, 72076 Tubingen, Germany

TABLE OF CONTENTS

1. Abstract
2. Introduction
3. Description of recent techniques to measure ocular parameters and visual function in mice
3.1. Measurement of refractive state by infrared photorefraction
3.2. Effects of mutations on refractive errors in mice
3.3. Measurement of corneal radius of curvature by photokeratometry
3.4. Pupillography during infrared photorefraction
3.5. Measurements of ocular dimensions by optical low coherence interferometry (OLCI)
3.6. Measurement of grating acuity and contrast sensitivity in an optomotor task
4. Acknowledgement
5. References

1. ABSTRACT

New techniques are described to measure refractive state, pupil responses, corneal curvature, ocular dimensions and spatial vision in mice. These variables are important for studies on myopia development in mice, but they are also valuable for phenotyping mouse mutants and for pharmacological studies.

2. INTRODUCTION

Although the mouse may not be considered a predominantly visual animal, its visual system is by no way vestigial. For instance, if scaled to body weight, its eye is even about 5 times larger than ours, and visual acuity found in behavioral tests is not very different from other animals with similar eye size (axial length little more than 3 mm, spatial resolution between 5 and 6 cycles/deg (1, 2). That the mouse visual system is worth a detailed investigation is also reflected in a large number of published papers (759 papers for the key words "mouse vision" in "Medline" as of June 2007). Furthermore, a major scholar book on mouse vision is about to be published (3). Also color vision is developed. Mammals are generally dichromatic with the exception of old world primates (and humans) - who are trichromatic. Also mice are dichromatic, with one receptor in the green range (509-512 nm) and the other in the near ultraviolet (360 nm). Based on these two receptors, and perhaps also using rod input, mice can be trained to discriminate isoluminant chromatic cues (e.g. 4).

The major advantages of the mouse as a model system for the understanding of visual processing include that (1) numerous knock-out models are available, (2) most advanced gene microarrays are availabe for the screening of the transcriptome, (3) the genome is completely

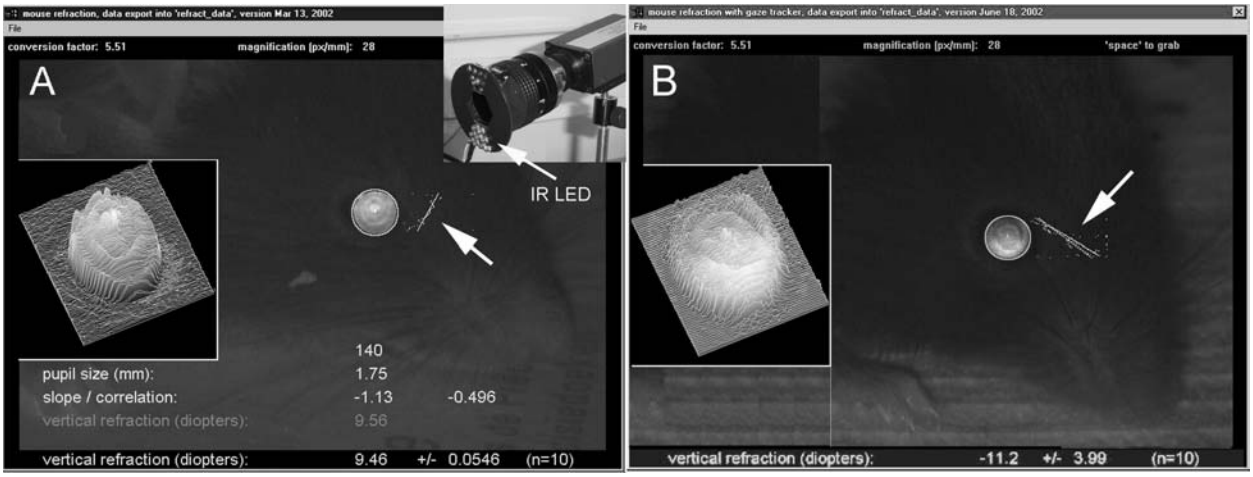

Figure 1. Infrared photorefraction in alert mice. The IR LED arrangement (see white arrow on the top in (A)) causes brighly illuminated pupils. The brightness gradient in the vertical pupil meridian can be fit by linear regression (see white lines, denoted by arrows, to the right of the pupils). The brightness distributions in the pupils (see 3D brightness profiles in the pupils on the left and brightness profile on the right of the pupils) are quite variable across the pupil in mouse eyes, suggesting poor optical quality. (A) hyperopic eye, (B) myopic eye (replotted after 8).

sequenced, (4) the mouse is the most extensively studied mammalian model for human diseases and considerable knowledge exists about biochemical pathways and pharmacology and, finally (5) mouse strains can be easily crossed and bred.

To be able to make full use of these advantages, problems of measuring biometrical parameters in a very small eye must be solved - the mouse eye is only little more than 3 mm long (e.g. 1, 5). Also, measuring visual function in mice is demanding. A number of new techniques are described below which are important in studies of ocular parameters and visual functions in mice.

3. DESCRIPTION OF RECENT TECHNIQUES TO MEASURE OCULAR PARAMETERS AND VISUAL FUNCTION IN MICE

3.1. Measurement of refractive state by infrared photorefraction

To follow the development of myopia in mice, some groups have used conventional streak retinoscopy (6, 7). However, it is difficult in a small pupil to see the direction of movement of a light bar, generated by light that returns after reflection from the fundus. Schmucker (*personal communication*, *2004*) found no significant correlation between the refractive states measured with white light streak retinoscopy and with automated infrared photoretinoscopy. on the other hand, a significant correlation was found between the power of trial lenses that were held in front of the eye, and the measurements by infrared photoretinoscopy. The existance of a correlation between lens power and measured refractions show that at least this technique can successfully measure refractive state in mouse eyes (8, 9).

The optical principle of automated infrared photoretinoscopy in human eyes has been described in detail by Schaeffel *et al* (10). In mice, an infrared sensitive video camera is positioned at about 60 cm distance from the mouse eye. Attached to the camera lens is an arrangement of infrared light emitting diodes (IR LED; see Figure 1A, white arrow in the top, right). A small fraction of the emitted light enters the pupil, is diffusely reflected from the backside layers in the fundus of the eye and returns to the camera. Because the IR LEDs are positioned directly below the camera aperture, they produce a brightly illuminated pupil - like the "red eye effect" seen with flash cameras. Furthermore, the brightness distribution in the vertical pupil meridian displays a gradient, with more light in the top in the case of a hyperopic eye (Figure 1A), and more light in the bottom in a myopic eye (Figure 1B). The measured brightness profiles are shown to the right of the pupils in Figures 1A and 1B, together with a linear regression line fit through the pixel brightness values (see arrows).

The refractions can be determined from the slopes of these regression lines. The only unknown variable is then the conversion factor from slope of the brightness profile in the vertical pupil meridian to refractive state. Using trial lenses of known optical power that are placed in front of the eye, the conversion factor can be determined (8).

The temporal sampling rate of this technique is determined by the video frame rate (analoge cameras: 25 Hz (PAL) or 30 Hz (NTSC), and 30 Hz or more with firewire cameras). The video image processing can easily be automated. As soon as the mouse appears in the field of view of the video camera, the image processing software detects its pupil (a simple task because it is brightly illuminated over the dark background of the fur). A custom-made image processing program then fits a linear regression through the pixel brightness values in the vertical pupil meridian and converts the measured brightness slope into refractive state.

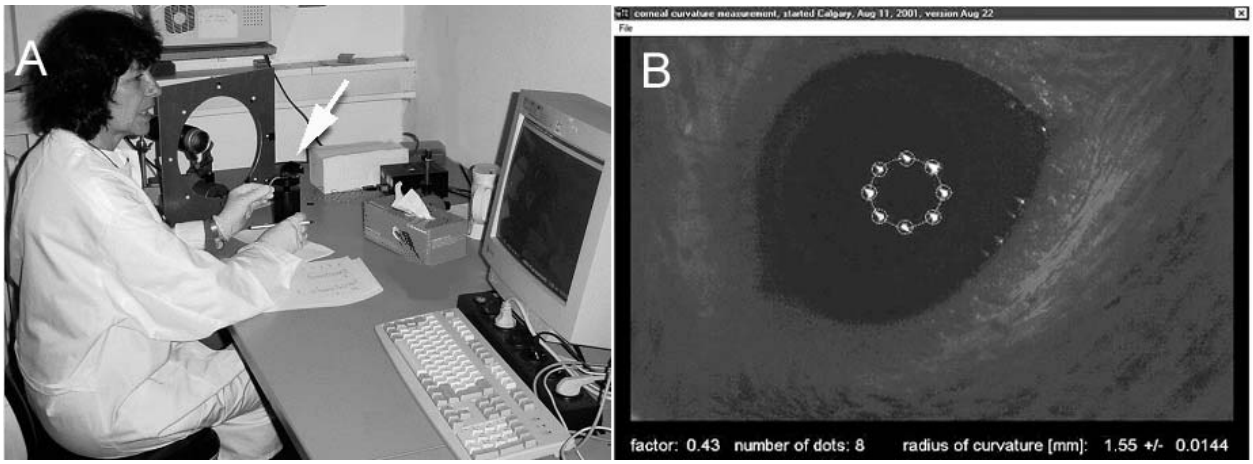

Figure 2. Infrared photokeratometry in alert mice. (A) The mouse (white arrow) is placed on a small platform and slightly restrained by holding its tail. The platform is moved back and forth until the infrared keratometer creates eight focused little light spots in the pupil (B). At the same time, the image processing software detects these spots and fits a circle through them. The diameter of the circle is proportional to the radius of curvature of the cornea. Calibration of the technique occurs by measuring a ball bearing of known radius of curvature.

Although this technique is very convenient to use, fast, and has a standard deviation of only about 2.7 diopters in the mouse eye, a few limitations have to be considered: (1) since mice have a deep excarvation at the place were the optic nerve leaves the eye (the optic disc), this area appears more myopic than the periphery. Therefore, to measure the refraction always at the same fundal area, the eye has to be aligned with the camera such that the first Purkinje image (a reflection of the infrared light source on the cornea) is about centered in the pupil, (2) although less hyperopia is measured with infrared photoretinoscopy than with white light streak retinoscopy (+20 D; +13.5 D; +15 D), one has to keep in mind that the light is reflected from the back of the eye not exactly from the phoptoreceptor layer but rather more anteriorly, mostly at the retino-vitreal interface (11, 7, 6). Therefore, eyes are generally measured "too short" and more hyperopic (the "small eye artifact" (12)). Even though the measured refractions appear usually hyperopic, this does not indicate that the mice are functionally hyperopic (8, 13). (3) The optical quality of the mouse eye is not very good as judged by the distribution of the light in the pupil during photorefraction (Figure 1) and by measurements of the optical wavefront aberrations with the Hartmann-Shack sensor (13). The average deviation of the measured wavefront from the perfect aberration free wavefront for the higher order aberration is 0.32+0.08 µm (with spherical and cylindrical refractive errors ignored). Nevertheless, it is clear that the optics of the mouse eye is so poor that it limits visual acuity - the final limits are imposed by neural factors (13). Both neural and optical factors generate a depth of focus of the mouse eye in the range of + 10 diopters. This means that the mouse visual acuity does not vary much between a few centimeters distance and infinity. The fact that a ciliary muscle and accommodation seem to be lacking is does not represent a problem (14). It is also clear that the large size of the crystalline lens would make any accommodative changes in shape and position very slow and little effective.

3.2. Effects of mutations on refractive errors in mice

Refractive development was studied in only a few mutants until now. Fernandez *et al* found that Nyxnob mice developed more deprivation myopia when they were treated with frosted transparent eye covers for a period of two weeks, than wildtype mice (9). Treatment with such googles produces myopia in most animal models (chicks, rhesus monkeys, tree shrews and guinea pigs - although wildtype mice (C57BL6) and DBA2 mice were found little responsive and developed rather variable amounts of myopia (15, 16, 17, 18, 9, 19, 7). Schippert *et al* found a mutant lacking a functional expression of the transcription factor Egr1 developed temporarily more myopic refractions between the age of 30 to 50 days (20). This myopia was at least partially axial since a more elongated eye was measured with the Zeiss AC Master (see below). A screening in 12 other mutants (largely affecting rhodopsin function and photoreceptor development) showed significant differences in refraction in several of them (Schaeffel & Seeliger, unpublished), but it has to be kept in mind that retinal thinning, induced by any kind of developmental disorder, places the light reflecting surface more back into the eye and produces a more myopic refractions - even though the external shape of the eye may remain unchanged. Studies measuring retinal thickness histologically and relating it to the previous refractive state *in vivo* could help to clarify this question.

3.3. Measurement of corneal radius of curvature by photokeratometry

For a more complete description of the optics of the eye, corneal radius of curvature is an important variable. Due the large difference in refractive indices between air and cornea tissue, the cornea provides generally more than 60 percent of the total power of the eye in air. Minor changes of curvature that could occur during drug treatment or due to mutations or strain differences have major impact on refractive state and vision.

Corneal radius of curvature can be measured in alert mice by placing them on a platform (Figure 2A, see

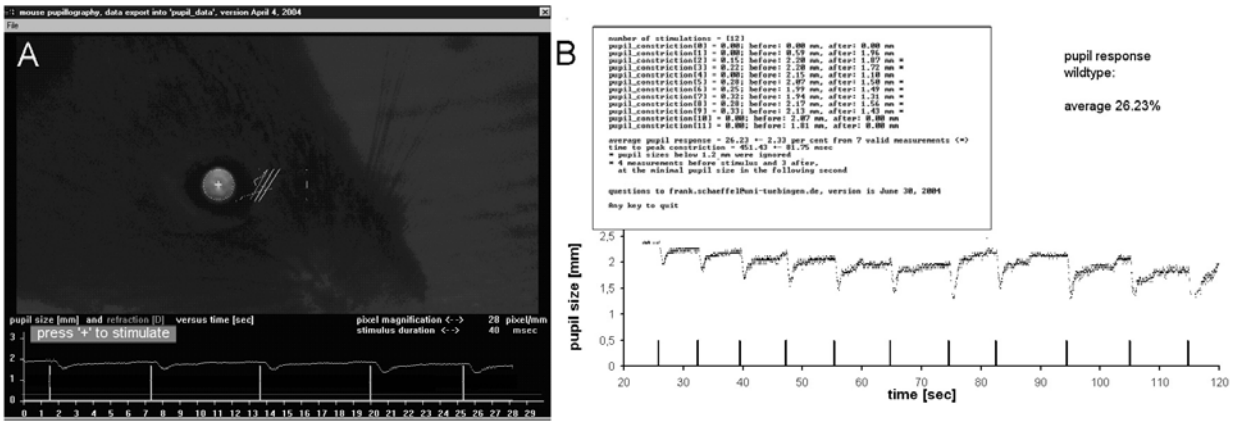

Figure 3. Pupillography during infrared photorefraction. (A) Since the pupil is tracked and measured during continuous photorefraction, its diameter can be plotted over time (see trace below the video frame). The light response is stimulated by flashing a green LED that is attached to the infrared photoretinoscope (see also top right in Figure 1A, where the green LED is visible above the camera aperture). (B) The pupil trace over time can be automatically analyzed by custom-made software (replotted from 23).

white arrow) and slightly restraining them by holding their tails. The platform is positioned at about 15 cm from a metal ring with a diameter of 300 mm that carries 8 IR LEDs (Figure 2A). The reflections of the IR LEDs on the corneal surface, the first Purkinje images, are also arranged in a circular pattern (Figure 2B). In a digital video image of the eye, the reflections can be detected by an image processing program and fit by a circle in real time (at 25 to 60 Hz, depending on the hardware platform). The diameter of the fitted circle is proportional to the curvature of the cornea - small circles for steep corneas with small radius of curvature, and larger circles for more flat corneas. For calibration, a ball bearing with known radius of curvature is measured. Since the diameters of the circle fit through the Purkinje images of the 8 LEDs and the diameter of the ball bearing are almost linearly related, a measurement in a single ball bearing is sufficient. The standard deviation of this procedure in alert mice is < 1% (< 5 diopters), with the major source of variability the depth of focus of the video camera. The video camera depth of field determines ultimatively how precisely the distance of the mouse to the keratometer and the camera can be controlled.

3.4. Pupillography during infrared photorefraction

Although recordings of electroretinograms provide detailed informations on the time courses of the retinal light responses, it remains unclear how much of this information reaches the brain (in this case, the pre-tectal areas which contains the sensory-motor interface of the pupillary light response). Therefore, measurements of pupil responses may not only reveal whether the retina responds to light stimulation but also whether the responses are transmitted through the optic nerve. It should be kept in mind, however, that light-induced pupil constrictions do not necessarily show rod and cone function since the pupil response is partially mediated by light-sensitive melanopsin-containing ganglion cells (e.g. 21).

In previous studies, pupils diameters were off-line analyzed in video frames (e.g. 22). Since the pupil of the mouse is detected and tracked during infrared photorefraction (Figure 1), it is easy to also use this technique for online analyses of pupil responses (23). For example, the effect of a single atropine eye drop on the mouse pupil was studied. To stimulate, a single green LED was attached to the infrared photoretinoscope and controlled by custom-made software that performed the infrared photorefraction (Figure 3A). The LED could be flashed via an USB to serial adapter by pressing the "Enter" key on the key board. The analysis of the pupil responses was automatically performed by custom-made software (Figure 3B). A result of this study was that the atropine-treated eyes displayed reduced pupillary light responses even after 220 hours (9 days) - impressively demonstrating how long-lasting the effects of atropine are on the pupil sphincter muscles in mouse eyes (23).

3.5. Measurements of ocular dimensions by optical low coherence interferometry (OLCI)

A major obstacle in experimental studies of myopia development in mice was that the ocular dimensions could not be measured by A-scan ultrasonography, as in most other experimental animal models (chick, monkey, guinea pig, tree shrew). Problems include that the ultrasound transducer probe can transmit only little energy into the eye because the steep curvature of the cornea results in only a small contact area, and that the ultrasound devices developed for the use in human eyes cannot resolve such short distances as in the mouse eye.

A progress was then that a optical low coherence interferometer, initially developed by Zeiss Meditec (Jena; http://www.meditec.zeiss.com/) to measure anterior chamber dimensions in human eyes (the Zeiss AC Master), turned out to be also useful for measuring the dimensions of mouse eyes (24, 25).

The optical principle of low coherence interferometry is based on a Michelson interferometer. A low coherence superluminescent laser diode (SLD) that

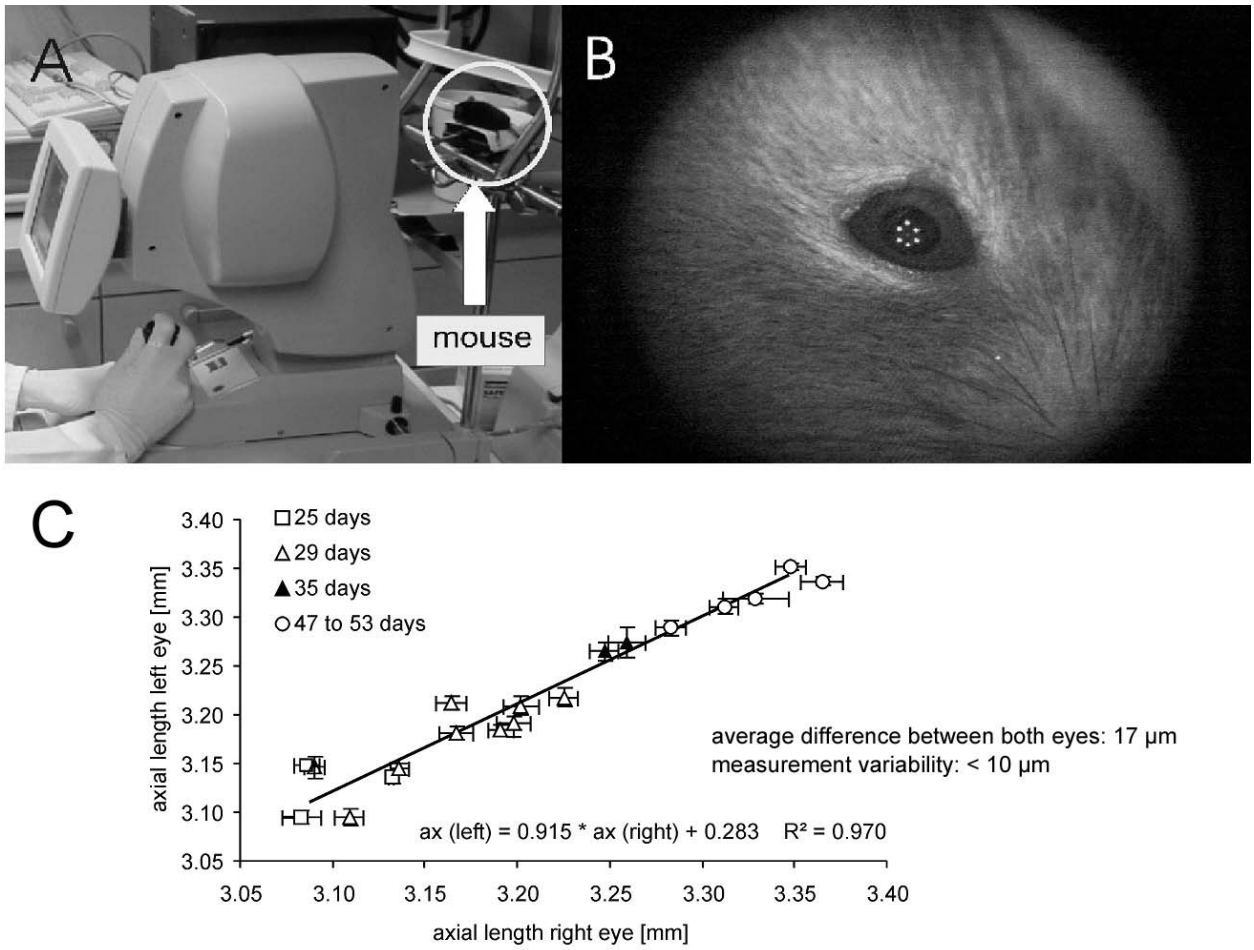

Figure 4. Optical low coherence interferometry in mouse eyes. (A) The slightly anesthetized mouse, positioned on an adjustable platform which is attached to the chinrest of the AC Master, is encircled. B. Close-up view used to adjust the eye in the measurement beam. The first Purkinje images of 6 infrared LEDs, built into the device, are used to align the eye. (C) Quality of the axial length data obtained with the AC Master - a plot of left versus right eyes (replotted after 24).

emits an infrared light with a peak emission at 850 nm and a half-band width of 10 nm serves as light source. Due to the broadened bandwidth, the coherence length is rather short (about 10 µm), compared to standard laser diodes, in which it is about 160 µm. The infrared laser beam emerging from the LED is divided into two perpendicular beams via a semi-silvered mirror. One part is transmitted through the semi-silvered mirror and reaches a stationary mirror. The other part reaches a second mirror that can be moved along the light path with high positional precision. After reflection from both mirrors, the two coaxial beams propagate to the eye, where they are reflected off from the cornea, the lens and the fundal layers. Interference between both beams can only occur when their optical path lengths are matched with extreme precision, within the coherence length. The occurrence of interference is detected by a photo cell and recorded as a function of the displacement of the movable mirror. Due to the usage of coaxial beams, the measurements are largely insensitive against longitudinal eye movements. The scanning time of the movable mirror is about 0.3 sec. In repeated measurements in mouse eyes, a standard deviation of 8 µm was found for axial length - equivalent to less than 2 diopters (24) (Figure 4).

It should be kept in mind that optical path lengths are measured with this technique which need to be converted into geometrical path lengths. This requires that the refractive indices for the ocular media are known. The problem has been analyzed by Schmucker & Schaeffel (24). The errors are generally small even if the refractive indices are not exactly known. Also, in most cases, differences are of interest between the treated and control eyes, rather than absolute axial lengths.

3.6. Measurement of grating acuity and contrast sensitivity in an optomotor task

There were several approaches to measure spatial visual performance in mice behaviorally. These approaches can be divided into three principles (1) recordings of visually evoked cortical responses (e.g. 26, 27, 28); (2) testing forced choice behavior in a swimming task, the "Visual Water Task, VWT" (29, 30, 31); (3) measuring the

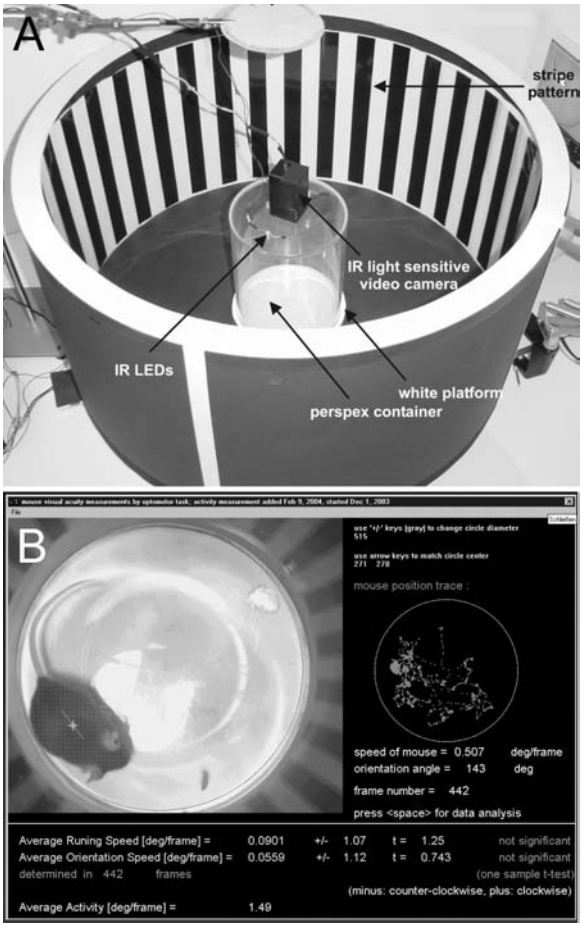

Figure 5. Automated optomotor drum for measuring whole body optomotor responses. (A) The mouse will be placed in a small inner perspex drum in the center of a larger drum which is inside covered with the square wave stripe pattern. The large drum is mechanically rotated by a DC motor. Both the center of mass of the mouse and the angular orientation of its body axis are automatically tracked by a video system (black arrow: small surveillance firewire camera that images the mouse, see also screen of the laptop). (B) The mouse is detected by locating pixels that are 40% below the average image brightness. The pixel center of mass is used for tracking of the mouse in the drum and an orthogonal regression through these pixels provides the body orientation axis. These variables are automatically statistically analyzed and compared to the direction of movement of the stripe pattern (replotted after 38).

optomotor response to drifting gratings that are either presented as printed on paper and attached to the inner wall of a rotating drum or, more sophisticated, presented on computer monitors that are arranged in a square (the "virtual optomotor system, VOS"). Different body movements, elicited by the drifting gratings, can be studied: head tracking (32, 33, 34, 35), optokinetic nystagmus of the eye (36, 37), or whole body optomotor responses (38, 20).

Approach (1) and (2) measure visual acuity for stationary targets, and (3) for moving targets. Processing of the two stimulations involve different brain areas. While acuity for stationary targets is largely determined by geniculo-cortical processing, moving targets are processed in the subcortical accessory optic system (39). Douglas *et al* have shown that ablation of the cortex did not change much the cut-off spatial frequency measured with the visual water task (VWT) and the virtual optomotor system (VOS), but the contrast sensitivity functions were changed (39). Contrast sensitivity was increased in the VOS but the range of high contrast sensitivity was found at lower spatial frequencies (contrast sensitivity about 20 at 0.05 cyc/deg with the VOS but only about 2 with the VWT). Another interesting aspect observed in the VOS was that tracking occurred only in the temporal-to-nasal direction for each eye, similar to the condition in infants (e.g. 40). This means that, depending on the direction of motion of the stripes, each eye can be independently tested (39). Despite that the stimulation set-up was very sophisticated and automatically compensated for changes in visual angles under which the freely moving mice saw the pattern, the experimenter had to make a perhaps partially subjective decision as to whether the mice responded or not.

Schmucker *et al* used the whole-body optomotor response with automated detection (Figure 5) to study the effects of ambient illuminance on grating acuity in C57BL6 wildtype mice (38). The whole body response is more "noisy" since it is contaminated by non-visual behaviors like cleaning behavior, or locomotor activity of the mouse while the pattern is ignored. Therefore, the standard deviations are larger and the measured grating acuity reached its limit at about 0.4 to 0.5 cyc/deg, slightly less than what was measured by Prusky *et al* in the VOS (33). However, since the experimenter cannot influence the data collection and its statistical analysis, the results are objective.

Results of this experimental approach include: optomotor acuity declined continuously when the illuminance (or luminance) was reduced: the "relative responses" were 100% at 400 lux (about 30 cd/m²), 76% at 40 lux (about 0.1 cd/m²), and 46% at 4 lux (about 0.005 cd/m²). A similar decline was not observed in an older study in the hooded rat where grating acuity at 1.2 cyc/deg remained similar between 3.4 and 0.0034 cd/m² in a three-choice discrimination apparatus (41). On the other hand, a newer study in mice found also an increase in spatial acuity with higher illuminances (34). That spatial vision improves so much with increasing illuminances is unexpected, given that the low f/number of the mouse eye must provide the retina with one of the brightest images of all vertebrates[5].

An analysis of the effects of mutations, leading to a loss of either rods or cones, or both, showed reduced visual acuity in cone-only models (0.10 cyc/deg in Rho -/- and 0.20 cyc/deg in CNGB1-/- compared to 0.30 cyc/deg in C57BL/6 wild-type mice). The "all-rod-mouse" (CNGA3 -/-) performed similarly in the optomotor test as the wild-type, both under photopic and scotopic conditions (38). This observation suggests that the rod system is not saturated, even at illuminances of 400 lux (about 30 cd/m²). It should also be kept in mind that rods represent about

95% of the photoreceptors in most vertebrates, including the mouse (42). Since the remaining 5% of cones are not clustered in a fovea but rather more evenly distributed across the retina, they may not reach a sampling density necessary for good spatial vision. In mice without any functional photoreceptors (CNGA3 -/- Rho -/-), no optomotor response could be elicited, suggesting that the light-sensitive, melanopsin-containing ganglion cells do not contribute to spatial vision (43).

4. ACKNOWLEDGEMENT

Preparation of this short review was partially supported by the German Research Council (DFG Scha 518-13/1). The review is based on a presentation at the DFG-sponsored meeting on "Vision and Cognition" in Wittenberg, Germany, on May 14-16, 2007. The author also thanks Prof. Jochen Graw, GSF Neuherberg, for the organization of the meeting.

5. REFERENCES

1. Remtulla S & PE Hallett: A schematic eye for the mouse, and comparisons with the rat. *Vision Res* 25, 21-31 (1985)
2. Gianfranceschi L, A Fiorentini & L Maffei L: Behavioural visual acuity of wild type and bcl2 transgenic mouse. *Vision Res* 39, 569-574 (1999)
3. Chalupa L & RW Williams (eds): Eye, Retina and Visual System of the Mouse, MIT Press, 2007. In press.
4. Jacobs GH, GA Williams GA & JA Fenwick JA: Influence of cone pigment coexpression on spectral sensitivity and color vision in the mouse. *Vision Res* 44, 1615-1622 (2004)
5. Schmucker C & F Schaeffel F: A paraxial schematic eye model for the growing C57BL/6 mouse. *Vision Res* 44, 1857-1867 (2004)
6. Beuerman RW, A Barathi, SR Weon & D Tan: Two models of experimental myopia in the mouse. *Invest Ophthalmol Vis Sci*, ARVO e-abstract 4338 (2003)
7. Tejedor J & P de la Villa P: Refractive changes induced by form deprivation in the mouse eye. *Invest Ophthalmol Vis Sci* 44, 32-36 (2003)
8. Schaeffel F, E Burkhardt, HC Howland & RW Williams: Measurement of refractive state and deprivation myopia in two strains of mice. *Optom Vis Sci* 81, 99-110 (2004)
9. Fernandes A, H Yin, AE Faulkner, PM Iuvone, RW Williams, F Schaeffel & MT Pardue: Mouse Model With ON Pathway Defect Has Increased Susceptibility to Form Deprivation Myopia. *Invest Ophthalmol Vis Sci*, ARVO e-abstract 2281 (2005)
10. Schaeffel F, H Wilhelm H & E Zrenner: Inter-individual variability in the dynamics of natural accommodation in humans: relation to age and refractive errors. *J Physiol* 461, 301-320 (1993)
11. Drager UC: Receptive fields of single cells and topography in mouse visual cortex. *J Comp Neurol* 160, 269-290 (1975)
12. Glickstein M & M Millodot: Retinoscopy and eye size. *Science* 168, 605-606 (1970)
13. de la Cera EG, G Rodriguez, L Llorente, F Schaeffel & S Marcos: Optical aberrations in the mouse eye. *Vision Res* 46, 2546-2553 (2006)
14. Woolf D: A comparative cytological study of the ciliary muscle. *Anatomical Record* 124, 145-163 (1956)
15. Wallman J, J Turkel & J Trachtman: Extreme myopia produced by modest change in early visual experience. *Science* 201, 1249-1251 (1978)
16. Smith EL 3rd LF Hung: Form-deprivation myopia in monkeys is a graded phenomenon. *Vision Res* 40, 371-381 (2000)
17. Siegwart JT Jr & TT Norton: The susceptible period for deprivation-induced myopia in tree shrew. *Vision Res* 38, 3505-3515 (1998)
18. Howlett MH & S McFadden: Form-deprivation myopia in the guinea pig (*Cavia porcellus*). *Vision Res* 46, 267-283 (2006)
19. Faulkner AE, MK Kim, PM Iuvone & MT Pardue: Head-mounted goggles for murine form deprivation myopia. *J Neurosci Methods* 161, 96-100 (2007)
20. Schippert R, E Burkhardt, M Feldkaemper, F Schaeffel: Relative axial myopia in Egr-1 (ZENK) knockout mice. *Invest Ophthalmol Vis Sci* 48, 11-17 (2007)
21. Zhu Y, DC Tu, D Denner, T Shane, CM Fitzgerald & RN Van Gelder: Melanopsin-dependent persistence and photopotentiation of murine pupillary light responses. *Invest Ophthalmol Vis Sci* 48, 1268-1275 (2007)
22. Pennesi ME, AL Lyubarsky & EN Jr Pugh: Extreme responsiveness of the pupil of the dark-adapted mouse to steady retinal illumination. *Invest Ophthalmol Vis Sci* 39, 2148-2156 (1998)
23. Schaeffel F & E Burkhardt E: Pupillographic evaluation of the time course of atropine effects in the mouse eye. *Optom Vis Sci.* 82, 215-220 (2005)
24. Schmucker C & F Schaeffel: *In vivo* biometry in the mouse eye with low coherence interferometry. *Vision Res* 44, 2445-2456 (2004)
25. Puk O, C Dalke, J Favor, MH de Angelis & J Graw: Variations of eye size parameters among different strains of mice. *Mamm Genome* 17, 851-857 (2006)
26. Porciatti V, T Pizzorusso & L Maffei: The visual physiology of the wild type mouse determined with pattern VEPs. *Vision Res* 39, 3071-3081 (1999)
27. Ridder WH 3rd & S Nusinowitz S: The visual evoked potential in the mouse--origins and response characteristics. *Vision Res* 46, 902-913 (2006)
28. Fischer QS, A Graves, S Evans, ME Lickey & TA Pham: Monocular deprivation in adult mice alters visual acuity and single-unit activity. *Learn Mem* 14, 277-286 (2007)
29. Prusky GT, PW West & RM Douglas: Behavioral assessment of visual acuity in mice and rats. *Vision Res* 40, 2201-2209 (2000)
30. McGill TJ, RD Lund, RM Douglas, S Wang, B Lu, BD Silver, MR Secretan, JN Arthur & GT Prusky: Syngeneic Schwann cell transplantation preserves vision in RCS rat without immunosuppression. *Invest Ophthalmol Vis Sci.* 48, 1906-1912 (2007)
31. Wong AA & RE Brown: Visual detection, pattern discrimination and visual acuity in 14 strains of mice. *Genes Brain Behav* 5, 389-403 (2006)

32. Thaung C, K Arnold, IJ Jackson & PJ Coffey: Presence of visual head tracking differentiates normal sighted from retinal degenerate mice. *Neurosci Lett* 325, 21-24 (2002)
33. Prusky GT, NM Alam, S Beekman & RM Douglas: Rapid quantification of adult and developing mouse spatial vision using a virtual optomotor system. *Invest Ophthalmol Vis Sci* 45, 4611-4616 (2004)
34. Abdeljalil J, M Hamid, O Abdel-Mouttalib, R Stephane, R Raymond, A Johan, S Jose, C Pierre & P Serge: The optomotor response: a robust first-line visual screening method for mice. *Vision Res* 45, 1439-1446 (2005)
35. Hart AW, L McKie, JE Morgan, P Gautier, K West, IJ Jackson & Cross SH: Genotype-phenotype correlation of mouse pde6b mutations. *Invest Ophthalmol Vis Sci* 46, 3443-3450 (2005)
36. Iwakabe H, G Katsuura, C Ishibashi, S Nakanishi: Impairment of pupillary responses and optomkinetic nystagmus in the mGlR6-deficient mouse. *Neuropharmacology* 36, 135-143 (1997)
37. Faulstich M, AM van Alphen, C Luo, S du Lac & CI De Zeeuw: Oculomotor plasticity during vestibular compensation does not depend on cerebellar LTD. *J Neurophysiol* 96, 1187-1195 (2006)
38. Schmucker C, M Seeliger, P Humphries, M Biel & F Schaeffel: Grating acuity at different luminances in wild-type mice and in mice lacking rod or cone function. *Invest Ophthalmol Vis Sci* 46, 398-407 (2005)
39. Douglas RM, NM Alam, BD Silver, TJ McGill, WW Tschetter & GT Prusky: Independent visual threshold measurements in the two eyes of freely moving rats and mice using a virtual-reality optokinetic system. *Vis Neurosci* 22, 677-684 (2005)
40. Valmaggia C, A Rütsche, A Baumann, C Pieh, Y Bellaiche Shavit, F Proudlock & I Gottlob: Age related change of optokinetic nystagmus in healthy subjects: a study from infancy to senescence. *Br J Ophthalmol* 88, 1577-1581 (2004)
41. Birch D & GH Jacobs GH: Spatial contrast sensitivity in albino and pigmented rats. *Vision Res* 19, 933-938 (1979)
42. Sterling P: How retinal circuits optimize the transfer of visual information. In: The Visual Neurosciences, Vol 1, Chalupa LM & JS Werner, eds., MIT press, Cambridge, Massachusetts, pp 234-259 (2003)
43. Hattar S, HW Liao, M Takao, DM Berson & KW Yau: Melanopsin-containing retinal ganglion cells: architecture, projections, and intrinsic photosensitivity. *Science* 295, 1065-1070 (2002)

Key Words : mouse, vision, eye growth, optomotor response, pupillography, refractive state, photorefraction

Send correspondence to: Frank Schaeffel, Section of Neurobiology of the Eye, University Eye Hospital, Calwerstrasse 7/1, 72076 Tubingen, Germany, Tel: 49-7071-2980739, Fax: 49-7071-295196, E-mail: frank.schaeffel@uni-tuebingen.de

New techniques are described to measure refractive state, pupil responses, corneal curvature, ocular dimensions and spatial vision in mice. These variables are important for studies on myopia development in mice, but they are also valuable for phenotyping mouse mutants and for pharmacological studies. Download full-text PDF. Source.